RJC

RASĀYAN *J. Chem.*
Vol. 17 | No. 4 |1910-1916| October - December | 2024
ISSN: 0974-1496 | e-ISSN: 0976-0083 | CODEN: RJCABP
http://www.rasayanjournal.com
http://www.rasayanjournal.co.in

EXPLORATION OF GEOPOLYMER BINDERS UTILIZING FLY ASH AND *SEWAGE SLUDGE* ACTIVATION: IMPACTS ON FRESH PROPERTIES, STRENGTH, DURABILITY, MICROSTRUCTURE AND THERMAL CONDUCTIVITY

Debabrata Dutta[1], Amit Shiuly[2], Sayani Roy[3], Debasis Sau [4,✉], Utpal Mandal[5] and Archan Majumder[6]

[1]Department of Civil Engineering, Ramkrishna Mahato Government. Engineering College, Purulia-723201(West Bengal), India
[2,4]Department of Civil Engineering, Jadavpur University, Jadavpur, Kolkata-700032 (West Bengal), India
[3]Independent Researcher, Rajpur Sonarpur(M), Kolkata-700149(West Bengal), India
[5]Department of Civil Engineering, Ramkrishna Mahato Government. Engineering College, Purulia- 723201 (West Bengal), India
[6]CEO, C A Construction, Kolkata-700129(West Bengal), India
✉Corresponding Author: debasissau67@gmail.com

ABSTRACT

This research aims to investigate the effect of the incorporation of *sewage sludge* as an activator in the formation of fly ash-based geopolymers. The geopolymer paste is made up of 15% *sewage sludge* by weight, with the remainder consisting of fly ash. The blended mix is activated using a hydroxide solution containing 10% Na2O relative to the total base material. To assess the mechanical and microstructural characteristics of the resulting geopolymer paste, it is necessary to conduct compressive strength tests as well as FESEM, SEM, XRD, and TG/DTA analyses. To evaluate the workability of the designed geopolymer paste, an area factor test can be used here. GPP4, using sodium silicate, achieved the highest 3-day compressive strength (38.0 MPa) with a dense, amorphous structure and minimal mass loss. In contrast, GPP3 with sludge showed a porous texture and moderate strength. TGA supports the observation of GPP4's amorphous nature, aligning with the findings from XRD and FESEM analyses. Further, sorptivity tests revealed changes in pore size and volume based on the activator and fly ash type. GPP4 also exhibited a thermal conductivity of 2.44×10^{-4} cal/cm/°C/s, demonstrating sludge's potential as an economical alternative for geopolymer binders.

Keywords: Fly Ash, Sludge, Activator Solution, Heat Curing, Strength, Durability, Microstructure

RASĀYAN*J. Chem.*, Vol. 17, No.4, 2024

INTRODUCTION

Waste generation has surged, posing disposal challenges, while cement production exacerbates CO_2 emissions. Utilizing waste materials for cement alternatives is crucial due to limestone scarcity. Geopolymers, pioneered by Joseph Davidovits, offer a sustainable solution. Derived from waste materials like fly ash and slag, and activated by alkaline solutions, geopolymers attract significant research interest as eco-friendly substitutes for ordinary Portland cement, curbing greenhouse gas emissions.[1] Geopolymer concrete offers a sustainable alternative to traditional cement, with fewer health hazards and pollution.[2] Extensive studies highlight its superior durability and sustainabilit[3-5] compared to conventional cement. Geopolymers, characterized by aluminium silicate structures, have an amorphous nature, unlike crystalline [6-8] zeolites. Nanocrystalline particles within geopolymer structures influence its properties, with synthesis conditions impacting crystallization. Factors such as curing temperature, activator type, and source material composition affect the formation of amorphous or crystalline structures.[10-16] In alkali-activated fly ash systems, hydroxide activators tend to produce crystals, while sodium ions favour of zeolite phase formation over potassium ions[7,14-15]. Increasing the amount of free water in mixing promotes zeolite synthesis.[10] Higher curing temperatures, from 45 to 65 °C, significantly enhance strength gain, with a ten-fold increase

http://doi.org/10.31788/RJC.2024.1748949

observed between 65 and 85°C [17]. Mild curing temperatures favour of zeolitic phase formation in alkali-activated fly ash systems.[11] Exposure of fly ash in geopolymer to an alkaline medium leads to rapid dissolution of its vitreous component, hindering crystallization.[18-20] However, zeolite phases may crystallize from dilute aqueous solutions under favourable conditions.[19] Slag, rich in CaO, decomposes under alkaline attack, resulting in the formation of calcium silicate hydrate (C-S-H) phases.[21] In highly alkaline solutions, metakaolin produces amorphous aluminosilicate, even in the presence of calcium compounds.[8,22] The presence of soluble calcium and silicate species in a neutral to mild pH environment supports the formation of C-S-H gel in basic geopolymer structures.[23] Silicate solution, the source of reactive silica, influences aluminosilicate polymerization.[24] However, the high water content (over 65%) in this solution contributes to the porous and semi-crystalline nature of geopolymers, leading to drying shrinkage issues over time.[25] Not all waste materials dissolve in alkali solutions[26], and geopolymer composition resembles zeolites but possesses complete amorphous characteristics[27]. Power-driven activation impacts geopolymer features under ambient heat exposure[28], while water plays a crucial role in calcined kaolin-based geopolymer synthesis.[29] While various studies have explored the use of different types of waste in geopolymers, there is limited research specifically focused on the incorporation of *sewage sludge*.[30-37] Therefore, in this study, Geopolymer concrete is explored with a focus on innovative activation solutions. Additionally, the utilization of fly ash-based Geopolymer binder in the presence of *sewage sludge* is investigated, addressing a gap in existing literature. Various tests, including slump, mechanical strength, durability (sorptivity, water absorption, apparent porosity), microstructure, and thermal conductivity, are conducted to evaluate the performance of casted geopolymer concrete.

EXPERIMENTAL

Material and Methods

Class C and F fly ash (ASTM C 618) and raw *sewage sludge* (semi-solid, pH 8.5-9.7) from Bidhannagar, Kolkata, India, were used. The sludge comprised 15% of the total mix with fly ash, aiming to reduce sodium silicate usage for a cost-effective and high-performance geopolymer product. First, fly ash and sludge (15% by weight) were hand-mixed in a partially wet state. An activator solution (Sodium silicate + Sodium hydroxide) was then added, and the mixture (Table-1) was blended for 5 minutes before being poured into cubical moulds. These were vibrated to remove air, covered with plastic to control evaporation, and rested for 1 hour. The specimens, labelled as GPP1 to GPP4 based on sodium silicate and sludge content, underwent heat curing at 75°C for 24 hours. Basic tests, including workability[38], compressive strength, water absorption, apparent density, porosity, sorptivity[34,39], and microstructural analyses (FESEM (Quanta FEG 250), SEM (QUANTA 2000), TG/DTA (Diamond TG/DTA; Perkin Elmer), XRD (Panalytical X'Pert Pro), will be conducted at relevant laboratories in Kolkata, India.

Table-1: Geopolymer Specimen Shapes and Geopolymer Paste Compositions

Specimen ID	Specimen Shape	Specimen Size	Class (Fly ash)	NaOH content of activator [wt.%]	$NaSiO_2$ Content of activator [wt.%]	Sludge [wt.%]	Water/ Fly ash
GPP1	Cubic	50mm×50 mm×50mm	ClassF	10	10	00	0.36
GPP2			ClassF	10	00	00	0.36
GPP3			ClassF	10	00	15	0.36
GPP4			ClassC	10	00	15	0.36

RESULTS AND DISCUSSION

Workability

Four series of fly ash-based geopolymer specimens were tested for workability in their fresh state using the polar graph method. GPP2 failed to form a gel without sodium silicate, crucial for polymerization. However, adding sludge improved workability even without sodium silicate. Specimen GPP3, activated with sludge, showed satisfactory performance. Calcium-based composites are likely formed during synthesis, enhancing the performance. This was noted that increasing slag reduces workability, a trend seen in Class C fly ash geopolymers activated with the sludge. Paste samples collected at intervals showed rapid phase changes, with a unit area factor marking the end of the plastic state.

Compressive Strength

Three sample series (GPP1, GPP3, and GPP4) were tested for compressive strength at the intervals of 3, 28, 60, and 90 days using a compression testing machine supplied by AIMEL as per ASTM C109. Results showed that compressive strength increased over time, likely due to slow synthesis and late precipitation within pores.[33-37,41] About 50% of non-blended fly ash geopolymers exhibited micro-cracks with aging. Calcium ions helped to form a stable geopolymer structure faster.[42] Specimen GPP4, made with Class C fly ash and sludge, showed the highest and most stable compressive strength, reaching 38 MPa at 3 days of curing. Sludge addition improved early-stage polymerization and maintained strength despite reduced the sodium silicate.

Water absorption and Apparent Porosity

Specimens GPP1, GPP3, and GPP4 were tested for apparent porosity (20.1, 23.1, and 17.2%) and water absorption (6.3, 6.9, and 4.2%) to gauge permeable pore volume using the weighting method. Porosity affects mechanical performance.[33-37] GPP3, with silicate replaced by sludge, showed a slight increase in porosity and water absorption. GPP4 had the lowest values, indicating better performance. Calcium compounds in an alkaline environment help form amorphous sodium aluminosilicate and secondary C-S-H gel, reducing pore size.[42] While Class F fly ash geopolymer with sludge showed moderate performance, overall Class C fly ash geopolymer with sludge performed exceptionally well.

Sorptivity

Specimens GPP1, GPP3, and GPP4 were tested for water sorptivity, a measure of water flow against gravity, indicating concrete durability as per ASTM C 1585-04. The test involved unidirectional water flow from the bottom surface. Water absorption per unit area was plotted against the square root of time to determine the sorptivity slope. GPP4 showed an initial increase in water absorption due to reduced average pore sizes, enhancing surface tension and capillary rise. However, GPP4 had the lowest total absorption, indicating changes in pore size and volume with different activating mediums and fly ash types.

SEM and FESEM

Scanning Electron Microscopy (SEM) and FESEM were used to examine morphological changes in fly ash-based geopolymers. GPP3 (Fig.-1) exhibited a more porous and rough texture with some unreacted material. Specimen GPP4, using sludge as an activator for Class C fly ash, showed a dense, well-connected amorphous structure with a smooth, compact surface (Fig.-2). No semi-crystalline or crystalline compounds were found in GPP4. FESEM analysis indicated the presence of secondary Ca-Al-Si structures, suggesting positive structural changes with Class C fly ash and sludge as the activator.[42]

XRD

XRD patterns (Fig.-3) revealed the mineralogical changes in Class F and Class C fly ash activated with sludge. Calcium supplements improve mineral characteristics, promoting the formation of polymeric structures. Specimen GPP3 (Fig.-3a) showed narrower, high-intensity peaks, indicating a mostly crystalline structure with inherent phases like quartz and mullite. In contrast, GPP4 (Fig.-3b) exhibited an almost completely amorphous phase, identified as Muscovite-3T, within the 2θ range of 5° to 140°. This amorphous nature suggests the higher reactivity and better geopolymerization, supporting the effective activation of Class C fly ash with sludge.

Thermo-Gravimetric Analysis (TGA)

TGA traces for specimens GPP3 and GPP4 showed thermal stability differences.[43] GPP3 (Fig.-4a) exhibited a sharp mass loss at ~100°C due to evaporation of water and an endothermic peak at 70-90°C.[44] Weight stabilized around 600°C, with 77.71% of the initial weight remaining. In contrast, GPP4 had only a 2.5% weight loss between 350 and 600°C, with 97.5% remaining at 600°C (Fig.-4b), indicating its more amorphous nature. These results align with XRD and FESEM analyses, confirming GPP4's having better geopolymer characteristics.

Application as a Geopolymer Binder

Calcium in Class C fly ash accelerates the formation of Ca-Al-Si amorphous structures during the initial phase of alkali activation with the sludge. As noted earlier, the high calcium content enhances

microstructure and hardened properties through the creation of Ca–Al-Si gel during polymerization, resulting in quick setting for Class C fly ash-based geopolymers.

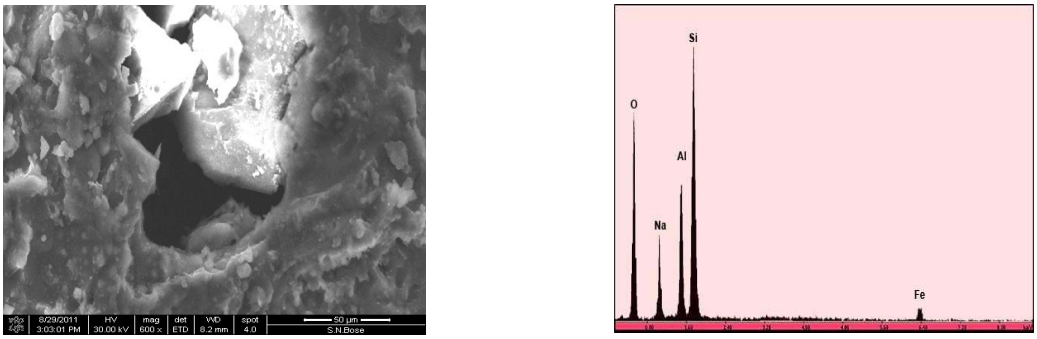

(a) (b)

Fig.-1: (a) SEM and (b) FESEM of GPP3

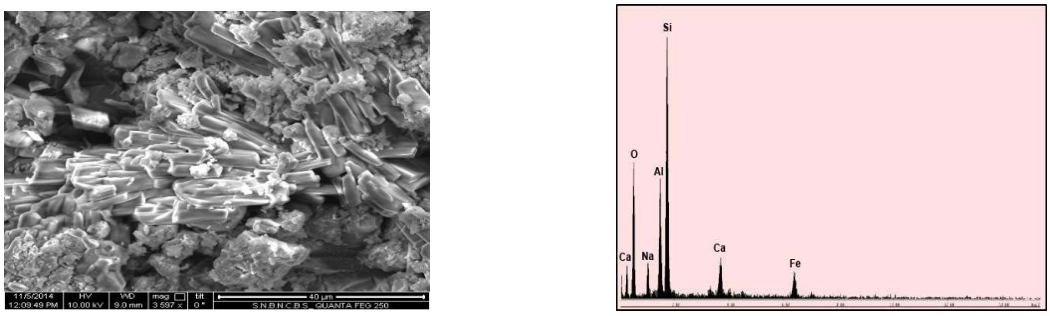

(a) (b)

Fig.-2: (a) SEM and (b) FESEM of GPP4

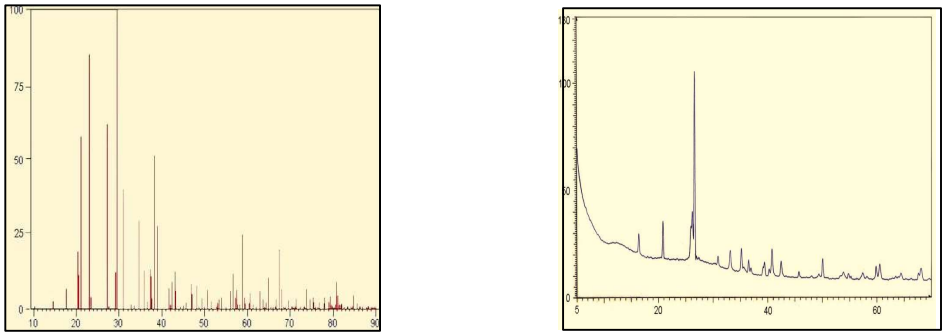

(a) (b)

Fig.-3: XRD of (a) GPP3 and (b) GPP4

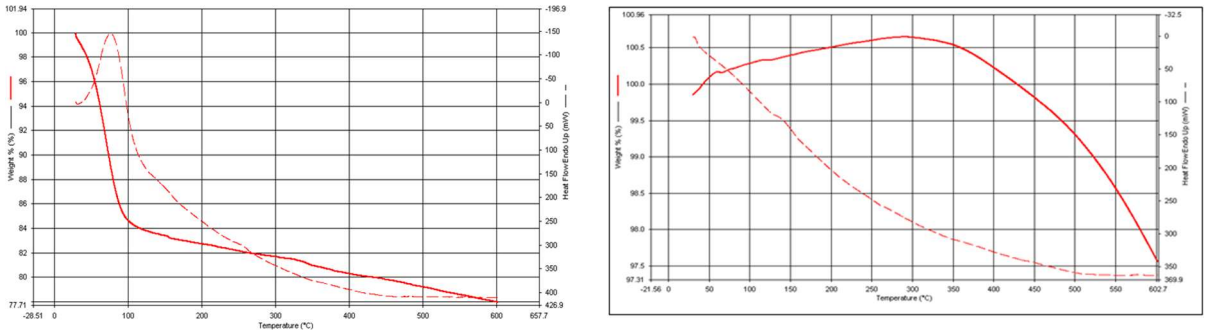

Fig.-4: TGA of (a) GPP3 and (b) GPP4

In this study, a 10 cm thick square and circular plate was developed incorporating 15 wt.% rice husks as a reinforcing material into the GPP4 mix for compressive strength and thermal conductivity respectively.

Compressive Strength and Thermal Conductivity

Ten cubic samples were tested to evaluate the effect of rice husk blending at 0 wt.%, 15 wt.%, and 30 wt.% with Class C fly ash in the GPP4 mixture (Class C fly ash activated with sludge). Thus, the compressive strength was measured at 3, 28, and 60 days to assess changes with aging. The addition of 15 wt.% rice husk as a reinforcing agent showed significant strength and stability in compressive strength for this blend was confirmed over time. This study investigates the thermal conductivity of roof tiles made from a GPP4 mix with rice husk as a reinforcing agent. The goal was to assess their potential as a sustainable building material characterized by moderate strength, low thermal conductivity, and high durability. Thermal conductivity was measured using Lee's method in the SKFGI physics department. This approach quantifies thermal conductivity (K) as the heat transfer per unit area across a temperature gradient in equation (1):

$$\frac{dQ}{dt} = K.A.\frac{\theta_2 - \theta_1}{d} \qquad (1)$$

Key parameters included cross-section area A, thickness d, and steady temperature θ_1 and θ_2. A cooling curve helps to determine the rate of change of temperature ($\frac{d\theta}{dt}$). The relationship for heat flow is refined to account for specific heat and geometry. The final equation (2) was made for the calculation of heat flow using the specific heat (s) of the standard material is noted as 0.089cal/°C. Where m- mass of the specimen and d' - change in thickness.

$$q = \left[\frac{m * s * \left(\frac{d\theta}{dt}\right) at(\theta = \theta_1) * \frac{r+2d'}{2r+2d'}}{\pi r^2 * (\theta_1 - \theta_2)}\right] * d \qquad (2)$$

The thermal conductivity was calculated using the above formulae. The thermal conductivity (GPP4) was measured at 2.44×10^{-4} cal/cm/°C/s. Manufacturing costs are minimal due to the low cost of raw materials like fly ash, sludge, and rice husk. The resulting product is suitable for roof tiles, offering strength, durability, thermal resistance, and cost-effectiveness.

CONCLUSION

The absence of sodium silicate inhibits polymerization in fly ash geopolymer (e.g., GPP2). Sludge addition improves workability even without sodium silicate (e.g., GPP3). Sludge exhibits similar activation potential to sodium silicate. Fresh alkali-activated Class C fly ash shows low workability. Aging increases strength in fly ash geopolymer due to internal pore pressure (e.g., GPP1). Sludge initiates polymerization akin to silica fume. Sodium silicate substitution by sludge yields moderate performance in Class F fly ash geopolymer. Class C fly ash geopolymer activated with sludge improves pore distribution. The sorptivity test indicates pore size and volume changes with activating medium and fly ash class. Sludge demonstrates effective activation for Class C fly ash. GPP3 shows a porous texture, while GPP4 displays a dense structure. GPP4 exhibits a well-connected amorphous structure. Structural improvements were observed in geopolymer with different fly ash and activator choices. GPP3 shows a predominantly crystalline structure. GPP4's crystalline phase largely converts to amorphous. GPP3 experiences mass loss due to water evaporation, while GPP4 shows minimal weight loss. TGA confirms GPP4's amorphous nature, consistent with XRD and FESEM results. Stability in strength was confirmed for the GPP4 specimen blended with 15% rice husk. GPP4 exhibits a maximum compressive strength (38.0 MPa) after 3-days of curing. The thermal conductivity of GPP4 was measured at 2.44×10^{-4} cal/cm/°C/s. The experimental investigation is aimed at developing a new trend of economic geopolymer binder with the betterment of structure at micro and macro levels. Thus, the effect of sludge as an alternative to commercial sodium silicate (initiator of polymerization) on the mechanical and microstructural properties of geopolymer paste based upon fly ash.

ACKNOWLEDGMENTS

The authors are thankful to the authorities of their institutions for the basic facilities provided by them.

CONFLICT OF INTERESTS

The authors report no potential conflicts of interest.

AUTHOR CONTRIBUTIONS

All authors made significant contributions to this manuscript, including reviewing, editing, and approving the final draft for publication. The research profiles of the two authors can be verified through their ORCID ids listed below:

Debabrata Dutta http://orchid.org/0000-0001-5761-2284
Amit Shiuly http://orchid.org/0000-0002-4942-3042
Sayani Roy http://orchid.org/0009-0000-3318-5388
Debasis Sau http://orchid.org/0000-0002-2508-6184
Utpal Mandal http://orchid.org/0009-0000-9147
Archan Majumder http://orchid.org/0009-0008-1195-8800

REFERENCES

1. D. N. Huntzinger, T. D. Eatmon, *Journal of Cleaner Production*, **17(7)**, 668(2009), https://doi.org/10.1016/j.jclepro.2008.04.007
2. R. A. Feely, C.L. Sabine, K. Lee, W. Berelson, J. Kleypas, B.J. Fabry, F.J. Millero, *Science*, **305(5682)**, 362(2004), https://doi.org/10.1126/science.1097329
3. P. K. Mehta, R. W. Burrows, Building Durable Structures in the 21st Century, *The Concrete Journal*, **23(3)**, 57(2001).
4. A. Castel, S. J. Foster, *Cement and Concrete Research*, **72**,48(2015), https://doi.org/10.1016/j.cemconres.2015.02.016
5. N. Ganesan, R. Abraham, S. Deepa Raj, and D. Sasi, *Construction and Building Materials*, **73**, 326(2014), https://doi.org/10.1016/j.conbuildmat.2014.09.092
6. P. D. Silva and K. S. Crenstil, *Cement and Concrete Research*, **38(6)**, 870(2008), https://doi.org/10.1016/j.cemconres.2007.10.003
7. J. L. Provis, G. C. Lukey, J. S. J. v. Deventer, *Chemistry of Materials*, **17(12)**, 3075(2005), https://doi.org/10.1021/cm050230i
8. S. Alonso, A. Palomo, *Materials Letters*, **47(1–2)**, 55(2001), https://doi.org/10.1016/S0167-577X(00)00212-3
9. R. A. Fletcher, K. J. D. MacKenzie, C. L. Nicholson, S. Shimada, *Journal of the European Ceramic Society*, **25(9)**, 1471(2005), https://doi.org/10.1016/j.jeurceramsoc.2004.06.001
10. D. W. Breck, J. Wiley, *Journal of Chromatographic Science*, **13(4)**, 18A(1975), https://doi.org/10.1093/chromsci/13.4.18A-c
11. A. F. Jiménez, A. Palomo, *Cement and Concrete Research*, **35(10)**, 1984(2005), https://doi.org/10.1016/j.cemconres.2005.03.003
12. W. M. Kriven, M. Gordon, J. L. Bell, *Microscopy and Microanalysis*, **10(S02)**, 404(2004), https://doi.org/10.1017/S1431927604886719
13. A. Palomo, M. T. Blanco-Varela, M. L. Granizo, F. Puertas, T. Vazquez, M. W. Grutzeck, *Cement and Concrete Research*, **29(7)**, 997(1999), https://doi.org/10.1016/S0008-8846(99)00074-5
14. N. Murayama, H. Yamamoto, J. Shibata, *International Journal of Mineral Processing*, **64(1)**, 1(2002), https://doi.org/10.1016/S0301-7516(01)00046-1
15. M. Inada, Y. Eguchi, N. Enomoto, J. Hojo, *Fuel*, **84(2–3)**, 299(2005), https://doi.org/10.1016/j.fuel.2004.08.012
16. J. L. LaRosa, S. Kwan, M. W. Grutzeck, *Journal of the American Ceramic Soceity*, **75(6)**, 1574(1992), https://doi.org/10.1111/j.1151-2916.1992.tb04228.x
17. Á. Palomo, S. Alonso, A. Fernandez-Jiménez, I. Sobrados, J. Sanz, *Journal of the American Ceramic Soceity*, **87(6)**, 1141(2004), https://doi.org/10.1111/j.1551-2916.2004.01141.x

18. A. Fernandez-Jimenez, I. García-Lodeiro, A. Palomo, *Journal of Materials Science*, **42(9)**, 3055(2007), https://doi.org/10.1007/s10853-006-0584-8
19. D. Khale R. Chaudhary, *Journal of Materials Science*, **42(3)**, 729(2007), https://doi.org/10.1007/s10853-006-0401-4
20. R. Terzano, M. Spagnuolo, L. Medici, B. Vekemans, L. Vincze, K. Janssens, P. Ruggiero, *Environmental Science & Technology*, **39(16)**, 6280(2005), https://doi.org/10.1021/es050079d
21. C. Panagiotopoulou, E. Kontori, T. Perraki, G. Kakali, *Journal of Materials Science*, **42(9)**,2967(2007), https://doi.org/10.1007/s10853-006-0531-8
22. S. Alonso A. Palomo, *Cement and Concrete Research*, **31(1)**, 25(2001), https://doi.org/10.1016/S0008-8846(00)00435-X
23. C. K. Yip, G. C. Lukey, J. S. J. v. Deventer, *Cement and Concrete Research*, **35(9)**, 1688(2005), https://doi.org/10.1016/j.cemconres.2004.10.042
24. E. Prud'homme, P. Michaud, E. Joussein, C. Peyratout, A. Smith, S. A. Clacens, J.M. Clacens, S. Rossignol, *Journal of the European Ceramic Society*, **30(7)**, 1641(2010), https://doi.org/10.1016/j.jeurceramsoc.2010.01.014
25. C. Kuenzel, L. J. Vandeperre, S. Donatello, A. R. Boccaccini, C. Cheeseman, *Journal of the American Ceramic Soceity*, **95(10)**, 3270(2012), https://doi.org/10.1111/j.1551-2916.2012.05380.x
26. J. G. S. V. Jaarsveld, J. S. J. V. Deventer, L. Lorenzen, *Minerals Engineering*, **10(7)**, 659(1997), https://doi.org/10.1016/S0892-6875(97)00046-0
27. H. Xu, J. S. J. V. Deventer, *International Journal of Mineral Processing*, **59(3)**, 247(2000), https://doi.org/10.1016/S0301-7516(99)00074-5
28. J. Temuujin, R. P. Williams, A. van Riessen, *Journal of Materials Processing Technology*, **209(12-13)**, 5276(2009), https://doi.org/10.1016/j.jmatprotec.2009.03.016
29. Z. Zuhua, Y. Xiao, Z. Huajun, C. Yue, *Applied Clay Science*, **43(2)**, 218(2009), https://doi.org/10.1016/j.clay.2008.09.003
30. M. A. Diab, *Journal of Engineering and Applied Science*, **69(1)**, 59 (2022), https://doi.org/10.1186/s44147-022-00111-6
31. K. Neupane, *Mechanics of Materials*, **103**, 110(2016), https://doi.org/10.1016/j.mechmat.2016.09.012.
32. M. Yadav, N. Saini, L. Kumar, V. N. Singh, K. Jagannathan, V. Ezhilselvi, *Civil Engineering*, **5(2)**, 537(2024), https://doi.org/10.3390/civileng5020028
33. J. Li, X. Dang, J. Zhang, P. Yi, Y. Li, *Polymers*, **15(2)**, 309(2023), https://doi.org/10.3390/polym15020309
34. Q. Han, P. Zhang, J. Wu, Y. Jing, D. Zhang, T. Zhang, *Nanotechnology Reviews*, **11(1)** ,1478(2022), https://doi.org/10.1515/ntrev-2022-0092
35. Y. Gao, K. Duan, S. Xiang, W. Zeng, *Frontiers in Materials*, 8(2021), https://doi.org/10.3389/fmats.2021.751585
36. Q. Fu, W. Xu, X. Zhao, M. Bu, Q. Yuan, D. Niu, *Ceramics International*, **47(21)**, 29550(2021), https://doi.org/10.1016/j.ceramint.2021.07.190
37. D. B. Istuque, L. Soriano, J. L. Akasaki, J. L. P. Melges, M. V. Borrachero, J. Monzó, J. Payá, and M. M. Tashima, *Construction and Building Materials*, **203**, 95(2019), https://doi.org/10.1016/j.conbuildmat.2019.01.093
38. D. Dutta, S. Ghosh, *Advances in Civil Engineering*, **2018(1)**, 1(2018), https://doi.org/10.1155/2018/2940169
39. P. A. Claisse, H. I. Elsayad, I. G. Shaaban, *Journal of Materials in Civil Engineering*, **9(3)**, 105(1997), https://doi.org/10.1061/(ASCE)0899-1561(1997)9:3(105)
40. H. Xu, J. S. J. v. Deventer, *Colloids and Surfaces A: Physicochemical and Engineering Aspects*, **216(1-3)**, 27(2003), https://doi.org/10.1016/S0927-7757(02)00499-5
41. W. K. W. Lee, J. S. J. V. Deventer, *Cement and Concrete Research*, **32(4)**, 577(2002), https://doi.org/10.1016/S0008-8846(01)00724-4
42. H. Xu, J. S. J. V. Deventer, *Minerals Engineering*, **15(12)**, 1131(2002), https://doi.org/10.1016/S0892-6875(02)00255-8
43. D. L. Y. Kong, J. G. Sanjayan, *Cement and Concrete Composites*, **30(10)**, 986(2008), https://doi.org/10.1016/j.cemconcomp.2008.08.001
44. P. Duxson, G. C. Lukey, J. S. J. V. Deventer, *Journal of Non-Crystalline Solids*, **352(52–54)**, 5541(2006), https://doi.org/10.1016/j.jnoncrysol.2006.09.019

[RJC- 8949/2024]